A Multi-Layer Phase Field Model for Extracting Multiple Near-Circular Objects*

Csaba Molnar[1], Zoltan Kato[1], Ian Jermyn[2]

[1]*Image Processing and Computer Graphics Department, University of Szeged, P.O. Box 652, 6701 Szeged, Hungary*

[2]*Department of Mathematical Sciences, Durham University, South Rd, DURHAM DH1 3LE, United Kingdom*

mcsaba@inf.u-szeged.hu, kato@inf.u-szeged.hu, i.h.jermyn@durham.ac.uk

Abstract

This paper proposes a functional that assigns low 'energy' to sets of subsets of the image domain consisting of a number of possibly overlapping near-circular regions of approximately a given radius: a 'gas of circles'. The model can be used as a prior for object extraction whenever the objects conform to the 'gas of circles' geometry, e.g. *cells in biological images. Configurations are represented by a multi-layer phase field. Each layer has an associated function, regions being defined by thresholding. Intra-layer interactions assign low energy to configurations consisting of non-overlapping near-circular regions, while overlapping regions are represented in separate layers. Inter-layer interactions penalize overlaps. Here we present a theoretical and experimental analysis of the model.*

1. Introduction

Object extraction is one of the key problems of image processing. The problem is simple to state: find the regions in the image domain occupied by a specified object or objects. It is, however, hard to solve: for all except the simplest images, solution requires object models containing significant shape information in addition to information concerning image properties. In addition, in many applications the number of instances of the object of interest occurring in the image may be unknown *a priori*, and the objects may interact: they may cluster together, be regularly spaced, or tend not to overlap, for example.

Most shape modelling methods use one or more template shapes and variations around them to capture shape uncertainty [1, 9, 8]. These methods are inefficient when the number of objects is unknown or when objects interact. Each object requires separate representation and computation, as well as auxiliary variables to achieve geometric invariance. Each pair of interacting objects requires extra computation. 'Higher-order active contour' (HOAC) models [7] provide an alternative approach. HOAC models can describe shape knowledge without templates, using long-range dependencies between region boundary points, and are intrinsically invariant. When expressed in terms of phase fields [6], they can be used to model configurations consisting of multiple interacting objects at no extra cost.

An important subset of object extraction problems involve multiple objects of near-circular shape, *e.g.* tree crowns in remote sensing images, and cells and other structures in biological images, and are thus difficult to solve using standard shape modelling methods. To address these problems, Horvath *et al.* [4, 3] described a HOAC model favouring subsets of the image domain consisting of any number of near-circular components with approximately a given radius. This 'gas of circles' (GOC) model was successfully used for the extraction of tree crowns from aerial images. The model suffers, however, from two limitations that render it unsuitable for many important applications. The first arises from the representation: because the configuration space consists of subsets of the image domain, as opposed to sets of subsets, touching or overlapping objects cannot be represented. The second arises from the model: the long-range interactions that favour near-circular shapes also create repulsive interactions between nearby objects, meaning that objects in low-energy configurations are typically separated by a distance comparable to their size. In [5], a first attempt was made to overcome these limitations in a binary Markov random field model. However, the use of binary variables means that the geometric accuracy of the representation is limited, and solution requires computationally expensive stochastic

*Partially supported by the grants CNK80370 of NIH & OTKA; the European Union and the European Regional Development Fund within the project TÁMOP-4.2.1/B-09/1/KONV-2010-0005.

optimization.

In this paper, we propose a generalization of the GOC model [3] that overcomes all these limitations while maintaining computational efficiency: the multi-layer phase field GOC model. This model consists of multiple instances of the phase field GOC model, each instance being known as a 'layer'. This makes it possible to represent overlapping objects as subsets on different layers, thereby removing the first limitation. The only inter-layer interaction is an overlap penalty: the long-range interaction does not act between different layers. As a result, objects in separate layers do not repel, thereby removing the second limitation. MAP estimates can be computed by minimizing the energy of the model via gradient descent, which is relatively computationally efficient. With a suitable data likelihood, the new model can be used for object extraction in the many cases in which the 'gas of circles' geometry is relevant. In this paper, we demonstrate its use for the extraction of cells and lipid droplets from biological images.

2. Single-layer 'gas of circles' phase field model

A phase field model [6] represents a subset $R \subset \mathcal{D}$ by a function $\phi : \mathcal{D} \to \mathbb{R}$ on the image domain $\mathcal{D}$, and a threshold t: $R = \{x \in \mathcal{D} : \phi(x) \geq t\}$. The single-layer 'gas of circles' phase field energy E is [3]:

$$E(\phi) = \int_{\mathcal{D}} \left\{ \frac{D_f}{2} |\nabla\phi|^2 + \alpha_f \left(\phi - \frac{\phi^3}{3}\right) + \lambda_f \left(\frac{\phi^4}{4} - \frac{\phi^2}{2}\right) \right\} - \frac{\beta_f}{2} \iint_{\mathcal{D}\times\mathcal{D}'} \nabla\phi\, \mathbf{G}(x, x')\, \nabla\phi' \ , \quad (1)$$

where (un)primed functions are evaluated at ($x \in \mathcal{D}$) $x' \in \mathcal{D}' \equiv \mathcal{D}$. The interaction function $\mathbf{G}$ is

$$\mathbf{G}(z) = \begin{cases} \frac{1}{2}\left(2 - \frac{|z|}{d} - \frac{1}{\pi}\sin\left(\frac{\pi(|z|-d)}{d}\right)\right) & \text{if } |z| < 2d \ , \\ 1 - H(|z| - d) & \text{else} \ , \end{cases} \quad (2)$$

where d controls the range of interaction and H is the Heaviside step function. This model assigns low energy to subsets of $\mathcal{D}$ consisting of a number of near-circular regions of approximately a given radius, separated by distances comparable to their size [3].

3. Multi-layer 'gas of circles' phase field model

We now extend the single-layer model of equation (1) to a *multi-layer* GOC model. The use of multiple layers enables the representation, not just of subsets, but of sets of subsets of $\mathcal{D}$, because subsets with non-empty intersection can now be represented on separate layers. As a result, the new model can represent objects that touch and overlap in the image.

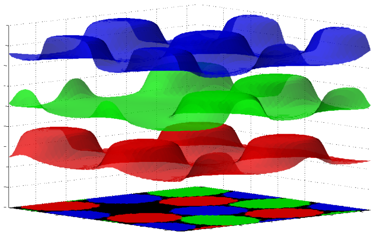

Figure 1. Layered phase fields

This is not enough on its own because the long-range interaction in equation (1) creates a repulsion between connected components, favouring configurations in which the objects are separated by a distance comparable to their size. While appropriate for some problems, *e.g.* tree crowns in regular plantations [3], it fails for problems in which objects are touching or overlapping, see *e.g.* Fig. 6. To overcome this limitation, in the new model the long-range interactions act intra-layer but *not* inter-layer. This has two effects. First, the low-energy configurations in each layer are still 'gas of circles' configurations, as required. Second, the repulsive interaction is eliminated, because repulsively interacting regions can 'escape' to separate layers. The result is that overlapping 'gas of circles' configurations on separate layers can now be combined without penalty. To avoid degenerate configurations, in which a given object is duplicated across all layers, an inter-layer area overlap penalty is introduced.

To proceed, we redefine the phase field as a multi-component object: $\phi = \{\phi_i\}_{i\in[1..\ell]} : [1..\ell] \times \mathcal{D} \to \mathbb{R}$, ϕ, where ℓ is the number of layers. The total energy $\tilde{E}$ of the new multi-layer model then takes the form

$$\tilde{E}(\phi) = \sum_{i=1}^{\ell} E(\phi_i) + \frac{\kappa}{4} \sum_{i\neq j} \int_{\mathcal{D}} (1+\phi_i)(1+\phi_j) \ , \quad (3)$$

where E is defined in equation (1), and κ is a new parameter controlling the strength of the overlap penalty. An example of a low-energy configuration is shown in Fig. 1.

Note that 'background' points, with $\phi_i \simeq -1$, do not generate overlap penalty. Note also that if they do not overlap, objects in range of the repulsive interaction will tend to lie in different layers. If they do overlap, there is competition between the repulsive interaction and the overlap penalty. If κ is not too large, they will exist on separate layers; if κ is large enough, they will exist on the same layer, perhaps reducing to one object.

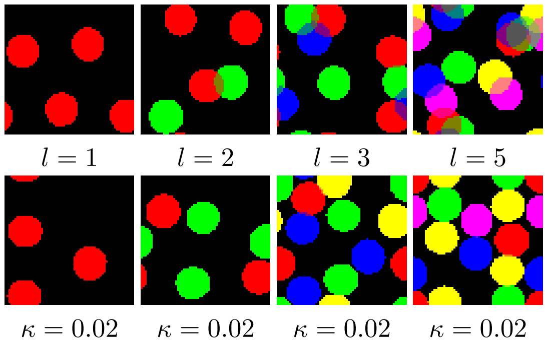

Figure 2. Typical configurations of the prior model ($r = 10$, negative circle energy). $\kappa = 0$ in the top row.

3.1 Functional derivative of the energy

The layered phase field energy will be minimized via gradient descent, for which we need to compute its functional derivative:

$$\frac{\delta \tilde{E}(\phi)}{\delta \phi_k(x')} = \frac{\delta E(\phi_k)}{\delta \phi_k(x')} + \frac{\kappa}{4} \frac{\delta E_O(\phi)}{\delta \phi_k(x')} \tag{4}$$

where $E_O(\phi)$ denotes the overlap energy term from Eq. (3). The first term is simply the functional derivative of E evaluated at the ϕ_k, and so is known [6, 3]. The derivative of the overlap energy is

$$\frac{\delta E_O(\phi)}{\delta \phi_k(x')} = 2 \sum_{i \neq j} \int_{\mathcal{D}} \delta_{ik}\, \delta(x, x')(1 + \phi_j(x)) \tag{5a}$$

$$= 2 \sum_{j \neq k} (1 + \phi_j(x')) \tag{5b}$$

$$= 2(\ell - 1) + 2 \sum_{j \neq k} \phi_j(x') \, . \tag{5c}$$

4. Experimental results

In this section, we report the evaluation of the behaviour of the multi-layer phase field GOC model on synthetic and real microscope images. For these experiments, we used the following phase field data term:

$$E_i(I, R) = \int_{\Omega} \Big\{ \gamma_1 \nabla I \cdot \nabla \phi + \gamma_2 \left[\frac{(I - \mu_{\text{in}})^2}{2\sigma_{\text{in}}^2} \phi_+ + \frac{(I - \mu_{\text{out}})^2}{2\sigma_{\text{out}}^2} \phi_- \right] \Big\} \, , \tag{6}$$

where: $\nabla \phi$, and $\phi_\pm = (1 \pm \phi)/2$ are approximately the normal vector to the boundary, and the characteristic functions of the region $(+)$ and its complement $(-)$ respectively [2]; $I : \mathcal{D} \to \mathbb{R}$ is the image data; $\mu_{\text{in,out}}$ and $\sigma_{\text{in,out}}$ are the parameters of pixel-wise Gaussian distributions modelling the image in the interior (in) and exterior (out) regions, learned from samples; and $\gamma_{1,2}$ are positive weights.

Fig. 2 shows some minimum energy configurations of the prior model. Without loss of generality, we chose $d = 10$, $\alpha_f = 0.2795$, $\beta_f = 0.0911$, $\lambda_f = 0.625$ and $D_f = 0.75$ to ensure the negative circle energy needed to have objects in the minimum energy configuration. As expected, $\kappa = 0$ yields overlapping objects, while $\kappa > 0$ prevents overlaps. If κ is too high, then either an empty configuration or unstable circles are produced.

In the next experiment, we take a closer look at the properties of the model in the case of two circles with different levels of overlap. We used two layers, circles of radius 10, and κ values in the range $[0, 1]$. Fig. 3 shows segmentation error versus κ and overlap w. Near $\kappa = 0.7$ there is a clear fall in the segmentation error. If $w > 10$, we need a larger κ to achieve a good segmentation.

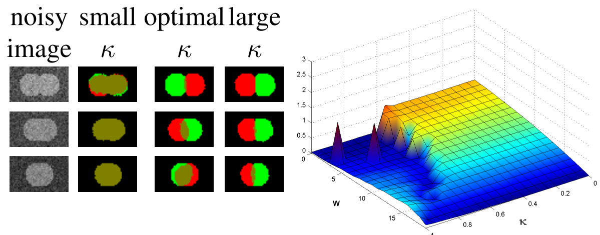

Figure 3. Segmentation results for noisy images containing two overlapping circles. Overlap w: 5 (top); 10 (middle); 15 (bottom). Small $\kappa = 0.55$; optimal $\kappa = 0.7$ (0.8 when $w = 15$); large $\kappa = 1$.

Finally, we examine the relationship between the data weight γ_2, overlap penalty κ, and extraction accuracy on synthetic images with more than two touching circles. Fig. 4 shows the ratio of correctly detected circles as a function of κ and γ_2. It is clear that there are several parameter pairs for which one can achieve a correct segmentation starting from a random initialization.

4.1. Biological application

In microbiology, one of the main image processing problems is to extract multiple objects, *e.g.* cells, lipid droplets, or other sub-cellular components, that are often near-circular with many overlaps. The light microscope techniques used produce noisy, blurred images

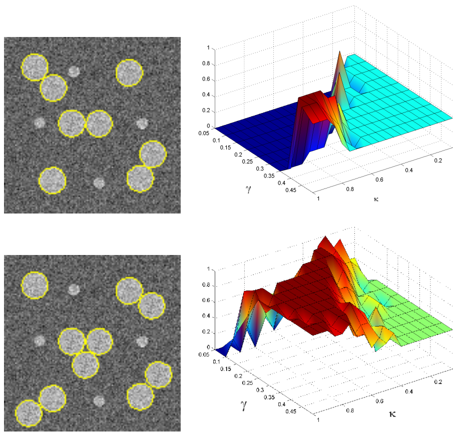

Figure 4. Results on synthetic images. Left: segmentation; right: proportion of correctly detected circles as a function of κ and γ_2.

with low contrast. The results shown in Fig. 5 and Fig. 6 show that the proposed model can solve these object extraction problems.

To initialize the multi-layer phase field, we used a simple thresholding and connected component detection, plus random assignment of different layers to nearby initial regions. Typical computation time in Matlab is about 20 seconds for a 200×100 image with 3 layers.

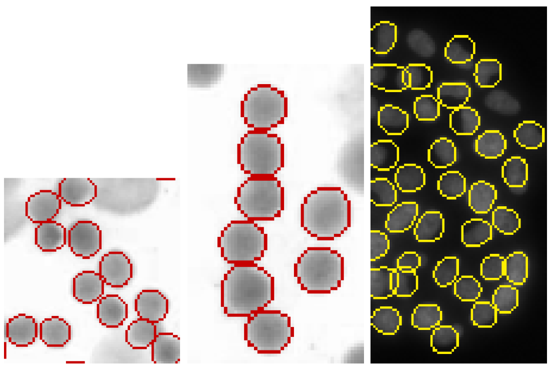

Figure 5. Extraction from light microscope images of cells having a particular radius.

5. Conclusions

The multi-layer phase field GOC model is capable of representing and modelling an *a priori* unknown number of touching or overlapping near-circular objects.

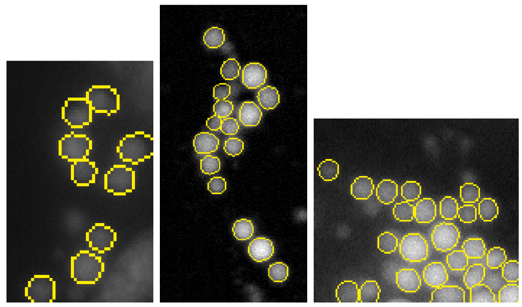

Figure 6. Extraction from light microscope images of lipid drops having a particular radius.

Such problems occur frequently in biomedicine and biology (*e.g.* cell images). Experiments show that the model behaves as expected, and that when coupled with an appropriate data model and initialization, can efficiently extract such object configurations from synthetic and real images.

References

[1] D. Cremers, F. Tischhauser, J. Weickert, and C. Schnorr. Diffusion snakes: Introducing statistical shape knowledge into the Mumford-Shah functional. *International Journal of Computer Vision*, 50(3):295–313, 2002.

[2] P. Horvath and I. Jermyn. A 'gas of circles' phase field model and its application to tree crown extraction. In *Proc. EUSIPCO*, Poznan, Poland, Sep 2007.

[3] P. Horvath and I. Jermyn. A new phase field model of a 'gas of circles' for tree crown extraction from aerial images. In *Proc. CAIP*, pp 702–709, Vienna, Austria, Aug 2007.

[4] P. Horvath, I. Jermyn, Z. Kato, and J. Zerubia. A higher-order active contour model of a 'gas of circles' and its application to tree crown extraction. *Pattern Recognition*, 42(5):699–709, May 2009.

[5] J. Nemeth, Z. Kato, and I. Jermyn. A multi-layer 'gas of circles' Markov random field model for the extraction of overlapping near-circular objects. In *Proc. ACIVS*, pp 171–182, Ghent, Belgium, Aug 2011.

[6] M. Rochery, I. H. Jermyn, and J. Zerubia. Phase field models and higher-order active contours. In *Proc. ICCV*, Beijing, China, IEEE, Oct 2005.

[7] M. Rochery, I. H. Jermyn, and J. Zerubia. Higher order active contours. *International Journal of Computer Vision*, 69(1):27–42, Aug 2006.

[8] C. Russell, D. Metaxas, C. Restif, and P. Torr. Using the P^n Potts model with learning methods to segment live cell images. In *Proc. ICCV*, pp 1–8. IEEE, Oct 2007.

[9] A. Srivastava, S. Joshi, W. Mio, and X. Liu. Statistical shape analysis: Clustering, learning, and testing. *IEEE Transactions on Pattern Analysis and Machine Intelligence*, 27(4):590–602, 2005.